

# A nuclear magnetic resonance study of poly(aryl ether ether ketone)

J. N. Clark\*, N. R. Jagannathan† and F. G. Herring

Department of Chemistry, The University of British Columbia, 2036 Main Mall,  
Vancouver V6T 1Y6, Canada

(Received 4 June 1987; revised 4 August 1987; accepted 13 August 1987)

Amorphous and crystalline samples of poly(aryl ether ether ketone) have been studied in the solid state by both  $^{13}\text{C}$  high-resolution cross-polarization/magic-angle spinning (CP/MAS) nuclear magnetic resonance (n.m.r.) and wide-line  $^1\text{H}$  n.m.r. The  $^{13}\text{C}$  spectrum was assigned using the dipolar dephased and variable-contact-time experiments. The CP/MAS spectrum of the amorphous sample displays much broader signals than does the crystalline sample. The  $^1\text{H}$  wide-line spectra were measured at temperatures from 295 to 440 K. The  $^1\text{H}$  spectra appeared as two superimposed signals having different spin-lattice relaxation times. At all temperatures below the glass transition, the lines of the crystalline spectra were wider and showed longer spin-lattice relaxation times than those of the amorphous spectra.

(Keywords: poly(aryl ether ether ketone); thermoplastic; magic-angle spinning; proton spin-lattice relaxation;  $^{13}\text{C}$  nuclear magnetic resonance;  $^1\text{H}$  nuclear magnetic resonance)

## INTRODUCTION

Poly(aryl ether ether ketone) (PEEK) is a semicrystalline aromatic polymer that is receiving ever-increasing commercial and academic attention. Marketed since 1981 by ICI, the primary application of the polymer is in the area of high-performance composite materials. Renowned for its excellent thermal stability and fine solvent resistance<sup>1</sup>, thermoplastic PEEK is an attractive alternative to the more conventional thermosetting resins used as the matrices for most fibre composites.

As with all semicrystalline polymers, the thermal and mechanical properties of PEEK are dependent upon the morphology and the thermal history of the material. There has been considerable interest in the current literature regarding the determination of the crystal structure and the characterization of the morphology. The principal techniques that have been employed are X-ray scattering<sup>2,3</sup> and thermal analysis<sup>4,5</sup>; also infra-red spectroscopy<sup>6</sup>, mechanical spectroscopy<sup>7,8</sup> and etching<sup>9</sup> have been used.

The use of nuclear magnetic resonance in the study of PEEK has been very limited<sup>10-12</sup>. One reason for this is the difficulty in doing solution n.m.r. due to the virtually insoluble nature of PEEK. Hence, characterization and other studies must be done in the solid state. In this paper we present the results of high-resolution  $^{13}\text{C}$  n.m.r. and wide-line  $^1\text{H}$  n.m.r. studies of PEEK. In addition to the conventional cross-polarization/magic-angle spinning (CP/MAS) experiment, the techniques of dipolar dephasing and variable contact time were employed to aid in assigning the spectrum and to make further distinction between the amorphous and the crystalline forms of PEEK. The proton work comprised two parts:

(a) a linewidth study and (b) a spin-lattice relaxation study, both as functions of temperature. Differential scanning calorimetry (d.s.c.) was also used as a complementary technique. The d.s.c. scans indicated the melting and glass transition temperatures.

The contrast of the results from the amorphous and crystalline samples provided insight into the molecular arrangements of the different morphologies.

## EXPERIMENTAL

### Materials

Both the amorphous and crystalline forms of PEEK were used as received from the suppliers. The crystalline resin was obtained indirectly from ICI Americas, Delaware, and the amorphous form from Westlake Plastics, Pennsylvania. The crystalline resin was in the form of a coarse grey powder of estimated crystallinity 35%<sup>13</sup>, and the amorphous sample was a translucent amber film.

### Differential scanning calorimetry

The differential scanning calorimetry was performed on a Mettler DSC-20 cell controlled by a TC-10A processor. Samples were heated at a rate of 10 K min<sup>-1</sup> from ambient to above the melting temperature. The crystalline material shows melting at 613 K.

### Nuclear magnetic resonance measurements

$^{13}\text{C}$  n.m.r. The spectrometer used for the high-resolution CP/MAS experiments was a Bruker CXP-200, operating at frequencies of 50.3 and 200.0 MHz for  $^{13}\text{C}$  and  $^1\text{H}$  nuclei, respectively. The conventional CP/MAS experiments were carried out following the pulse sequence reported in the literature<sup>14</sup>. A Delrin rotor was used and the sample spinning rates were 3-4 kHz. External fields of 40 G for the  $^{13}\text{C}$  nuclei and 10 G for the protons were required for spin-locking, to obtain the Hartmann-Hahn condition<sup>15</sup>. The magic angle was set

\* Department of Chemical Engineering and Chemical Technology, Imperial College, London SW7 2BY, UK

† Present address: Department of Chemistry, Colorado State University, Fort Collins, CO 80523, USA

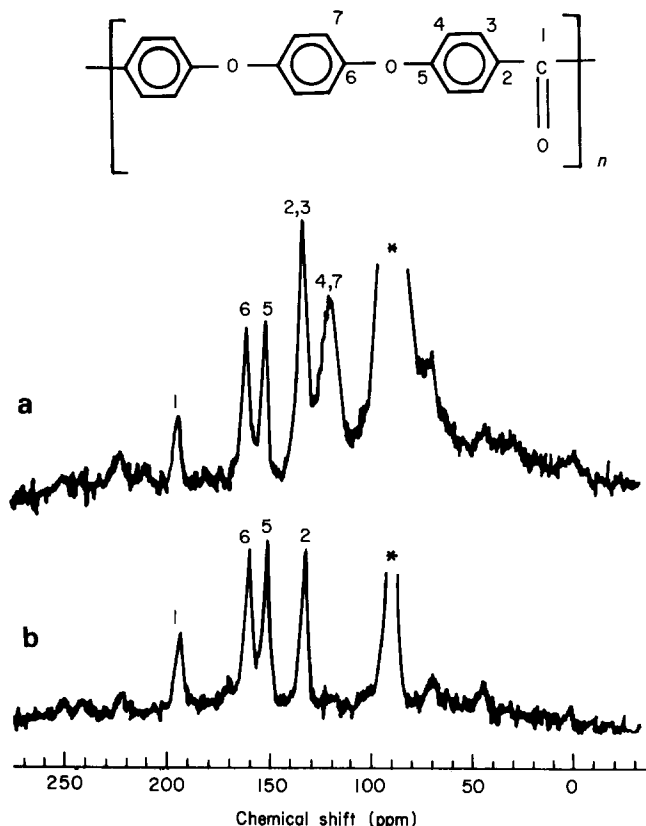


Figure 1 (a) Conventional CP/MAS  $^{13}\text{C}$  spectrum of crystalline PEEK. (b) The dipolar dephased spectrum of PEEK (delay =  $40\ \mu\text{s}$ ). (The asterisk denotes the signal due to Delrin)

following the method of Frye and Maciel<sup>16</sup>, using powdered KBr packed underneath the sample. Phase alternation was used throughout to eliminate baseline and intensity artifacts. Typically over 1000 transients were collected per spectrum.

The dipolar dephasing experiments required the introduction of the  $40\ \mu\text{s}$  delay time directly following the proton  $90^\circ$  pulse, and preceding the decoupling pulse<sup>17</sup>. During this delay time, the magnetization of the protonated carbons decays much faster than that of the non-protonated carbons. The variable-contact-time CP/MAS spectra for both the crystalline and amorphous forms of PEEK were obtained by varying lengths of cross-polarizing contact times from 0.05 to 5 ms.

$^1\text{H}$  n.m.r. The same spectrometer was employed for the proton study and the spectra were collected in quadrature with block size of 2K and sweep width of 500 000 Hz. For each spectrum, 16 to 32 transients were averaged. An inversion recovery pulse sequence ( $180-\tau-90$ ) was used to measure spin-lattice relaxation times. The recycle time was larger than  $5T_1$  and spectra for 10 to 15 delay times were obtained for each sample. The temperature range extended from 295 to 440 K and the temperature was controlled to  $\pm 1\ \text{K}$ .

## RESULTS

### $^{13}\text{C}$ nuclear magnetic resonance

Figure 1a presents spectra of the conventional high-resolution CP/MAS spectrum of crystalline PEEK. Figure 1b shows the dipolar dephased spectrum of the same material. Note that the broad intense signal at

119 ppm present in Figure 1a is not seen in the dephased spectrum. Also the intensity of the signal at 133.2 ppm is reduced to about half in Figure 1b.

Figure 2 contrasts the high-resolution spectra of the crystalline and amorphous forms of PEEK, under the same spectrometer conditions. The linewidths of the amorphous spectrum are at least twice those of the crystalline one for all carbons.

An example of the variable-contact-time results is presented in Figure 3, as a plot of the relative intensity of

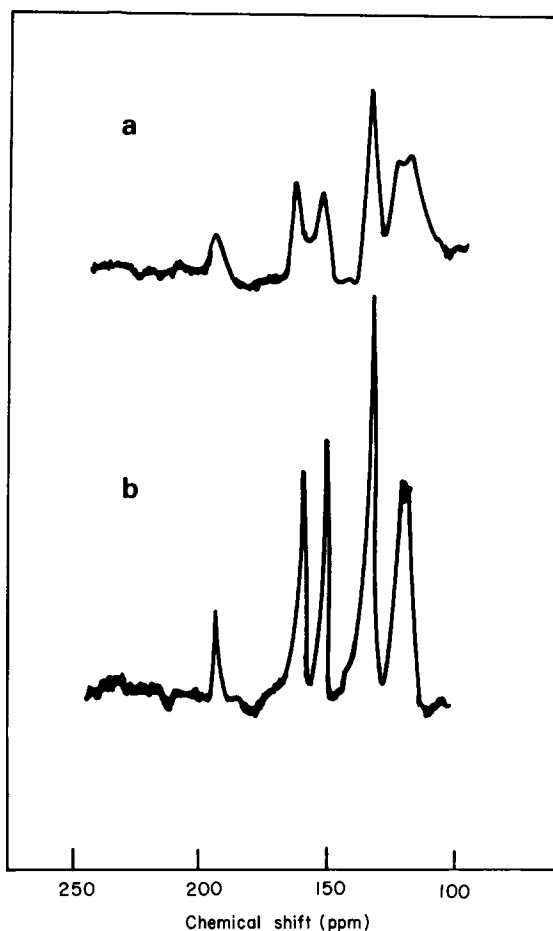


Figure 2 Solid-state  $^{13}\text{C}$  CP/MAS spectra of (a) amorphous PEEK and (b) crystalline PEEK

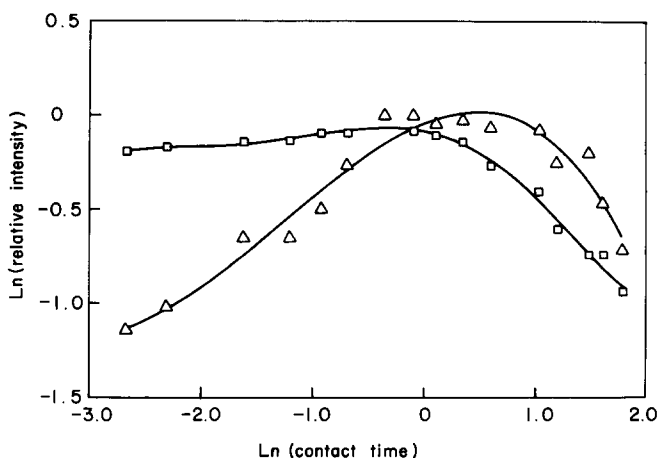
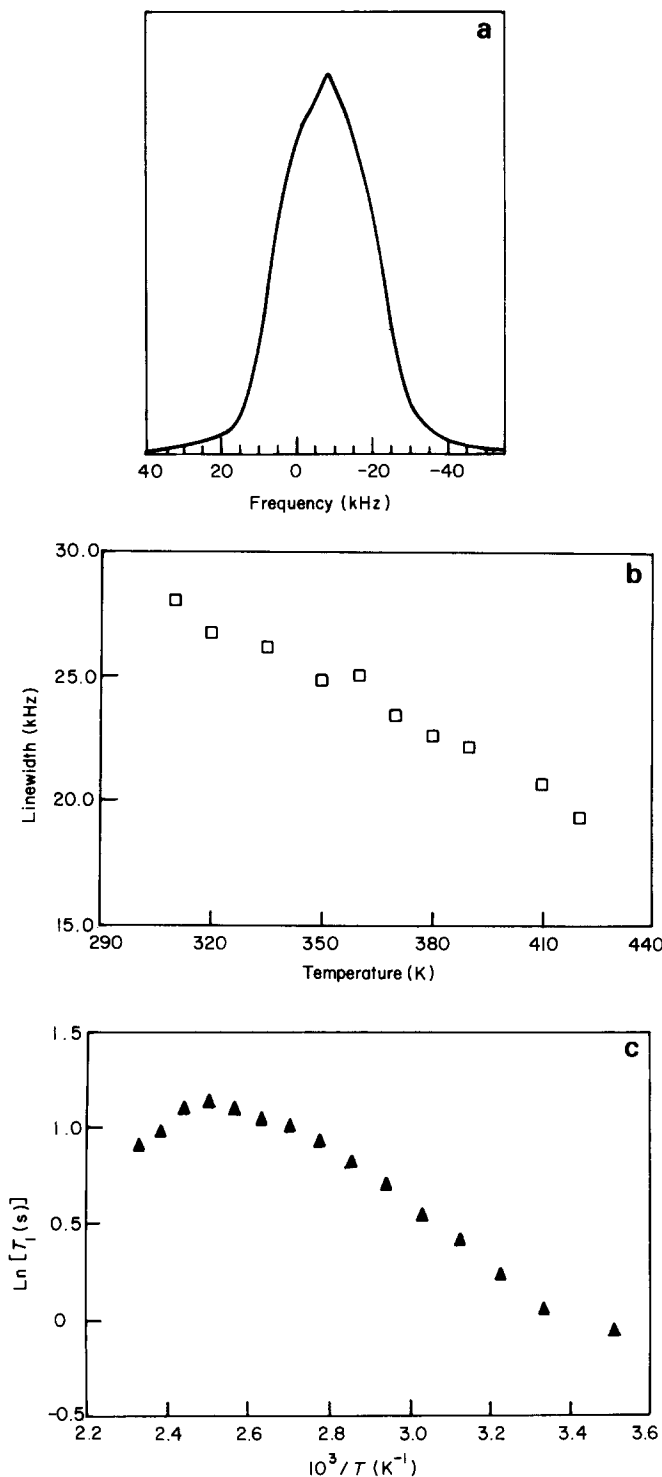


Figure 3 Variable-contact-time plots for amorphous PEEK: C3, C4 protonated carbons ( $\square$ ); C6 non-protonated carbon ( $\triangle$ )



**Figure 4** (a) Wide-line  $^1\text{H}$  spectrum of crystalline PEEK. (b) Linewidth versus temperature for  $^1\text{H}$  spectra of crystalline PEEK. (c)  $\ln T_1$  (relaxation time) versus inverse temperature for amorphous PEEK

the signal against the contact time for protonated and non-protonated carbons for amorphous and crystalline samples. The magnetization of the protonated carbons is at maximum value at shorter contact times than for the quaternary carbons. Relative to the crystalline material, the optimum contact time for all the amorphous carbons is shorter.

#### $^1\text{H}$ nuclear magnetic resonance lineshapes

At ambient temperature, the  $^1\text{H}$  spectra appeared as

broad Gaussian lines with a small narrow component at the approximate centre of the Gaussian line; this is illustrated in *Figure 4a*. The linewidth appeared to be inversely proportional to the temperature (see *Figure 4b*). The behaviour of the amorphous spectra is different from the crystalline in two respects: (i) the amorphous spectral lines are narrower than the crystalline ones and (ii) at the glass transition point, the amorphous linewidth drops abruptly, narrowing by 3 kHz.

#### Proton $T_1$ relaxation

Proton spin-lattice relaxation times were calculated using a three-parameter fit equation developed by Levy and Peat<sup>18</sup>. The room-temperature spin-lattice relaxation times are, for the crystalline 1.35 s and for the amorphous 0.98 s. Throughout the temperature range (300–430 K) the crystalline relaxation time is longer than the amorphous. *Figure 4c* shows a plot of  $T_1$  and temperature. The lower-temperature portion of the curve is linear. The relaxation time is at a maximum value at approximately  $T_g$ , declining again at higher temperatures. From the linear portion of the curves an activation energy may be obtained; it is  $13.3 \text{ kJ mol}^{-1}$  for both the crystalline and the amorphous samples.

The relaxation times represent the relaxation of the bulk sample, dominated by the behaviour of the Gaussian component. This relaxation is the sum of two relaxations, one from the broad Gaussian and one from the narrow signal superimposed. This was most clearly observed in partially relaxed spectra where the Gaussian signal was yet negative and the narrow, fast relaxing line was already positive. At all temperatures the narrow component did show a shorter relaxation rate.

## DISCUSSION

#### $^{13}\text{C}$ nuclear magnetic resonance

The assignment of different carbons in the high-resolution CP/MAS spectrum was made with the aid of the dipolar dephased spectrum, which distinguished between protonated and non-protonated carbons, and by referring to model compounds. Details of the assignment are as explained in ref. 12. Complete assignments are as shown in *Figure 1*.

Comparing the spectra (*Figure 2*) of the amorphous and crystalline samples, we note that the amorphous lines are significantly broader. This is contrary to the immediate expectation; in an early CP/MAS work on polymers the broader spectral lines were incorrectly thought to be due to crystallinity<sup>19</sup>. Subsequent work, however, indicated that amorphous polymers do exhibit broader lines<sup>20,21</sup>. Two factors may be responsible for the broadening of the amorphous lines: (i) heterogeneous broadening due to a wider distribution of chemical shifts present in the amorphous material and (ii) homogeneous broadening caused by molecular motion at frequencies comparable to the decoupling field.

The variable-contact-time experiment also produced results contrary to expectation, in that the optimum contact time for the crystalline sample was longer than for the amorphous one. But care must be taken in comparing contact times because cross-polarization rates are sensitive to the spectrometer conditions, particularly the Hartmann-Hahn condition. Some of the scatter seen in

the data is due to drift of the spectrometer frequencies over the course of a long experiment (Figure 3). Thus, it was necessary to repeat the experiments to ascertain that the results were reproducible, dependent on the sample and independent of spectrometer settings.

Protonated carbons show shorter optimum contact times than quaternary carbons because of the more efficient transfer of magnetization from the adjacent hydrogens; the variable-contact-time experiments confirmed the dipolar dephasing experiment.

The comparison of results for the amorphous and crystalline samples is of greater interest: the crystalline samples require longer contact times to achieve optimum signal intensity. This is somewhat surprising because strong dipolar interactions promote cross-polarization and dipolar interactions are likely to be stronger in the more dense and less mobile crystalline material. But there is a second factor that effects the cross-polarization behaviour, the spin-lattice relaxation time of the protons in the rotating frame ( $T_{1\rho}$ ). The  $T_1$  of the amorphous PEEK is shorter on account of the greater molecular motion relative to the crystalline. The shallowness of the positive slope of the intensity versus contact time plot for the protonated carbon of the amorphous sample suggests two opposing factors: (i) the increase of the  $^{13}\text{C}$  magnetization with time and (ii) the decrease in magnetization that follows the decay of the proton magnetization.

#### $^1\text{H}$ nuclear magnetic resonance

The two-component nature of the wide-line proton spectra arises from the presence of two sorts of molecular motion. The broad component of the signal is due to the protons that are rigid in the lattice, and the narrow component is due to the more mobile protons.

Below  $T_g$ , the narrow component of PEEK tends to be slightly more intense in the spectra of the amorphous form than in the crystalline spectra. The reason for this could be that the reduced density of the amorphous material allows greater mobility of chain segments than is possible in the crystalline form.

The effect of additional mobility in the amorphous sample is also seen in the broad component, which is less wide in the amorphous sample than in the crystalline. Linewidth is most sensitive to motions in the  $5 \times 10^4$  to  $3.3 \times 10^6$  Hz range<sup>22</sup>.

As the temperature increases, the broad component continues to narrow gradually due to the progressive increase in thermal motions. The abrupt narrowing of the amorphous line at the glass transition is explained by the onset of cooperative motions of large segments of the macromolecular chains. Unfortunately, the experimental limits on the temperature were such that the maximum temperature obtainable was only 20°C above  $T_g$ ; the effect of the temperature further above the  $T_g$  could not be observed.

Second-moment calculations are often made instead of linewidth measurements. But, because the Gaussian linewidth is proportional to the square root of the second moment, the two methods yield similar results<sup>23</sup>. Difficulties were encountered in obtaining the second-moment values from these data. These were (i) the loss of initial points during the receiver recovery time and (ii) uneven baselines, which caused incorrect contributions

from the spectral wings; hence linewidth data were used for our discussions.

The crystalline morphology generally exhibits a longer relaxation time than the amorphous form and a similar behaviour was noted for other macromolecules reported in the literature<sup>24</sup>. The amorphous material relaxes more quickly because of the increased motion of the polymer chains relative to the more rigid crystalline structure, where the molecular motion is constrained by the crystallites.

Normally the  $T_1$  value of a polymer is thought to be a minimum at the glass transition temperature but in this work  $T_1$  is a maximum at  $T_g$  (as measured by d.s.c.). The discrepancy is accounted for by noting the high operating frequency of the spectrometer. A  $T_1$  minimum indicates the temperature at which  $\omega\tau_c \approx 1$  (where  $\omega$  is frequency and  $\tau_c$  is correlation time). For the 200 MHz field, the correlation time at which  $T_1$  is minimal would be approximately  $5 \times 10^{-9}$  s; such a fast motion would only be prominent at considerably higher temperatures.

## CONCLUSIONS

Crystalline and amorphous samples of poly(aryl ether ether ketone) have been examined in the solid state by high-resolution  $^{13}\text{C}$  CP/MAS and wide-line  $^1\text{H}$  n.m.r.

The high-resolution  $^{13}\text{C}$  spectrum was assigned with the aid of model compounds and the dipolar dephased spectrum. The spectrum of the amorphous material was much broader than that of the crystalline material, although no chemical shift was observed. The CP/MAS variable-contact-time experiment indicated that the optimum contact time for the amorphous sample was shorter than for the crystalline sample. This is due to the faster spin-lattice relaxation ( $T_1$ ) of the protons in the amorphous sample, rather than to stronger dipolar interactions.

The wide-line  $^1\text{H}$  spectra revealed an interesting feature: two components, a broad intense signal approximately Gaussian in shape and a much less intense narrow signal at the centre of the broad. At all temperatures these lines displayed different relaxation times, the narrow one being shorter. The narrow signal may be due to the end groups of the molecules or to low-molecular-weight oligomers present in the material.

## ACKNOWLEDGEMENTS

The authors would like especially to thank Dr A. L. MacKay of the Department of Physics, University of British Columbia, for many helpful discussions and also Dr Greg Louma for bringing PEEK to our attention. This work was funded by the Department of National Defence (Canada) and the Natural Sciences and Engineering Research Council of Canada. J.C. also expresses her thanks to Polysar Ltd for a graduate research scholarship.

## REFERENCES

- 1 Woodhams, R. T. *Polym. Eng. Sci.* 1985, **25**, 562
- 2 Kumar, S., Anderson, D. P. and Adams, W. W. *Polymer* 1986, **27**, 329
- 3 Fratini, A. V., Cross, E. M., Whitaker, R. B. and Adams, W. W. *Polymer* 1986, **27**, 861

- |   |  |
|---|--|
| <p>4 Cebe, P. and Hong, S. <i>Polymer</i> 1986, <b>27</b>, 1183</p> <p>5 Kemish, D. J. and Hay, J. N. <i>Polymer</i> 1985, <b>26</b>, 905</p> <p>6 Nguyen, H. X. and Ishida, H. <i>Polymer</i> 1986, <b>27</b>, 1400</p> <p>7 Richardson, A., Ania, F., Rueda, D. R., Ward, I. M. and Balta Calleja, F. J. <i>Polym. Eng. Sci.</i> 1985, <b>25</b>, 355</p> <p>8 Sasuga, T. and Hagiwara, M. <i>Polymer</i> 1986, <b>27</b>, 821</p> <p>9 Olley, R. H., Bassett, D. C. and Blundell, D. J. <i>Polymer</i> 1986, <b>27</b>, 344</p> <p>10 Bishop, M. T., Karasz, F. E., Russo, P. S. and Langley, K. H. <i>Macromolecules</i> 1985, <b>18</b>, 86</p> <p>11 Whitaker, R. B., Attalla, A., Sullenger, D. B., Wang, P. S., Dichairo, J. V. and Kenyon, A. S., 16th National SAMPE Tech. Conf., 1984, p. 361</p> <p>12 Clark, J. N., Jagannathan, N. R. and Herring, F. G. <i>Polym. Commun.</i> 1985, <b>26</b>, 329</p> | <p>13 Cogswell, F. N. and Hopprich, M. <i>Composites</i> 1983, <b>14</b>, 251</p> <p>14 Yannoni, C. S. <i>Acc. Chem. Res.</i> 1982, <b>15</b>, 201</p> <p>15 Hartmann, S. R. and Hahn, E. L. <i>Phys. Rev.</i> 1962, <b>128</b>, 2042</p> <p>16 Frye, J. S. and Maciel, G. E. <i>J. Magn. Reson.</i> 1982, <b>48</b>, 125</p> <p>17 Opella, S. J. and Frey, M. H. <i>J. Am. Chem. Soc.</i> 1979, <b>101</b>, 5854</p> <p>18 Levy, G. C. and Peat, I. R. <i>J. Magn. Reson.</i> 1975, <b>18</b>, 500</p> <p>19 Veeman, W. S., Menger, E. M., Ritchey, W. and de Boer, E. <i>Macromolecules</i> 1979, <b>12</b>, 924</p> <p>20 Sefcik, M. D., Schaefer, J., Stejskal, E. O. and McKay, R. A. <i>Macromolecules</i> 1980, <b>13</b>, 1132</p> <p>21 Bunn, A., Cudby, M. E. A., Harris, R. K., Packer, K. J. and Say, B. J. <i>Polymer</i> 1982, <b>23</b>, 694</p> <p>22 McBrierty, V. J. <i>Polymer</i> 1974, <b>15</b>, 503</p> <p>23 Schlik, S. and McGarvey, B. R. <i>Polym. Commun.</i> 1984, <b>25</b>, 369</p> <p>24 Tanka, H. <i>J. Appl. Polym. Sci.</i> 1982, <b>27</b>, 2197</p> |
|---|--|